Ultrasound and computed tomography features of primary acinic cell carcinoma in the parotid gland: A retrospective study

Jia Li [a,1], Xia Gong [a,1], Ping Xiong [a,*], Qiuhua Xu [a], Yu Liu [b], Yazhu Chen [c], Zhen Tian [d]

[a] Department of Ultrasound, Shanghai Ninth People's Hospital, School of Medicine, Shanghai Jiao tong University, Shanghai, PR China
[b] Department of Radiology, Shanghai Ninth People's Hospital, School of Medicine, Shanghai Jiao tong University, Shanghai, PR China
[c] Department of Biomedical Engineering, Shanghai Ninth People's Hospital, School of Medicine, Shanghai Jiao tong University, Shanghai, PR China
[d] Department of Pathology, Shanghai Ninth People's Hospital, School of Medicine, Shanghai Jiao tong University, Shanghai, PR China

ARTICLE INFO

ABSTRACT

Objective: The aim of this study was to characterize the ultrasound (US) and computed tomography (CT) findings of primary acinic cell carcinoma (AciCC) of the parotid gland.
Subjects and methods: Seventy patients (70 lesions) with histopathologically proven AciCC underwent US or CT examination. The following characteristics were assessed on US images: size, shape, border, echogenicity, echotexture, internal structure, distal acoustic enhancement, and vascularity. The following characteristics were evaluated on CT images: size, shape, border, density, CT values on plain and contrast-enhanced scans, enhancement pattern, enhancement degree, and surrounding bone destruction.
Results: On US images, lesions were irregular, well-defined, hypoechoic, heterogeneous, and poorly vascularized. On CT images, lesions were regular and well-defined, and showed slight heterogeneous enhancement.
Conclusion: These findings suggest that most primary AciCCs show benign features on US and CT.

1. Introduction

Acinic cell carcinoma (AciCC) is a relatively rare malignancy of ductal cell origin that represents 1–6% of salivary gland neoplasms [1], and often occurs in the parotid gland. It is considered to be the third most common epithelial malignancy of the salivary glands in adults, and the second common in children. AciCC is more predominant in the female population, with a female-to-male ratio of 1.5:1 [2]. AciCC can be caused by previous radiation exposure [3] and familial predisposition [4]. The role of estrogen receptors, progesterone receptors, and androgen receptors has been reported in some cases of AciCC, which indicated hormonal regulation in the development of AciCC. Moreover, genetic alterations at chromosomes 4p, 5q, 6p, and 17p have been associated with AciCC of the parotid gland. To our knowledge, surgery along with adjuvant postoperative radiotherapy usually has satisfactory results. The prognosis of AciCC is good, with the survival rate ranging from 55% to 89% [5–7]. The local recurrence rate is 8–56% [8], and the 10-year and 20-year survival rates are 88% and 83% [9].

FNAC is highly sensitive for the diagnosis of salivary gland lesions. The pathological diagnosis depends on identifying cells that demonstrate significant acinar cell differentiation. Immunohistochemical staining of this tumor is not specific and does not play an important diagnostic role. Imaging modalities such as ultrasound (US) and computed tomography (CT) are frequently used to assess tumors of the parotid gland. However, because of the low prevalence of AciCC, there are only a few reports on US and CT findings for AciCC in the English literature. Our study aimed to describe the features of primary AciCC of the parotid gland and the use of US and CT in order to try to improve the diagnostic accuracy.

2. Materials and methods

2.1. Patients

This retrospective study was approved by the Ethics Committee of the hospital. The study population included a total of 117 consecutive patients with histopathologically proven primary solitary AciCC of the parotid gland who consulted our hospital between

* Corresponding author at: Department of Ultrasound, Shanghai Ninth People's Hospital, School of Medicine, Shanghai Jiao tong University, 639 Zhizaoju Road, Huangpu, Shanghai, PR China. Tel.: +86 021 37701292; fax: +86 021 23271101.

E-mail addresses: xpyxpy2011@163.com (J. Li), gongxiafeng@163.com (X. Gong), xiongpxp@163.com (P. Xiong), xu_qiu_hua@msn.com (Q. Xu), 13917266194@126.com (Y. Liu), yazhuchen@sjtu.edu.cn (Y. Chen), tian0304_cn@163.com (Z. Tian).

[1] Co-first author.

Table 1
Patient characteristics.

Cases (*N*)	117
Gender	
Male (*n*)	54
Female (*n*)	63
Age	
Average	44.9
Minimum	9
Maximum	84
Examinations	
US only	35
CT only	22
US and CT	13

US, ultrasound; CT, computed tomography.

December 2003 and August 2012. The patients included 54 men and 63 women with a mean age of 44.9 years (SD, 16.12; age range, 9–84 years). Among the 117 patients, 70 (70 lesions) underwent preoperative US or CT examination: 35 underwent only US; 22, only CT; and 13, US and CT. Of the 117 tumors, 59 were located in the left parotid gland while the remaining tumors were on the right side. Table 1 summarizes the patients' characteristics and the imaging modality used. The diagnosis of AciCC was confirmed after surgical resection of the tumor and histological analysis of the tumor tissue.

2.2. Imaging methods

2D US was performed using GE-Voluson E8 (GE Healthcare, Austria) or DU-5 (Branson, Italy), with a 10-MHz linear-array transducer. CT was performed using a 16-section scanner (GE Medical Systems; 120 kV potential, 200 mA current, 5 mm contiguous slice thickness) or a MDCT 64-row scanner (Philip Brilliance 64; 140 kV potential, 50 mA current, 0.63 contiguous slice thickness). The scan range was from the external auditory canal to the thorax. For contrast-enhanced images, a bolus intravenous dose of 80 ml (OptiVantage^{TM} DH) of nonionic contrast agent was injected at a rate of 2.5 ml/s via a power injector. For contrast-enhanced CT, the time delay was 40 s.

The images were first retrospectively reviewed independently by two radiologists, and the imaging examinations were then reviewed in a final consensus interpretation by the same two radiologists. The following characteristics were assessed on US images: size, shape, border, echogenicity, echotexture, internal structure, distal acoustic enhancement, and vascularity. The following characteristics were evaluated on CT images: size, shape, border, density, CT values on plain and contrast scans, enhancement pattern, enhancement degree, and surrounding bone destruction.

2.3. Evaluation of image findings

The size of lesions was considered to be the maximal length of the transversal section. The shape of the lesions was determined to be regular (round, oval) or irregular. Irregular shape also included a lobulated appearance. The border of lesions was evaluated as well-defined or ill-defined. The echogenicity of lesions was evaluated by comparing the echogenicity of the lesion with that of the surrounding normal parotid gland tissue. Based on their echogenicity, the lesions were classified as isoechoic, hypoechoic, and mixed-echoic. No hyperechoic lesions were found in any of the patients. Both the echotexture from US images and density from CT images were evaluated as homogeneous or heterogeneous. Heterogeneous lesions were classified under cyst, calcification, or mixed-echogenicity area. Color Doppler ultrasonography set to the same pulse repetition frequency as the US techniques was used to assess the distribution and displacement of intratumor vessels. If three or more than three vessels were detected, the lesions were regarded

Table 2
Summary of US imaging findings.

Features	Variables	*n* (%)
Size		2.2 ± 0.63 cm
Shape	Regular	19 (40%)
	Irregular	29 (60%)
Border	Well-defined	38 (79%)
	Ill-defined	10 (21%)
Echogenicity	Isoechoic	1 (2%)
	Hypoechoic	35 (73%)
	Mixed-echoic	12 (25%)
Echotexture	Homogeneous	4 (8%)
	Heterogeneous	44 (92%)
Liquid areas	Present	15 (31%)
Calcification	Present	1 (2%)
Posterior echo	Enhancement	25 (52%)
	Without enhancement	23 (48%)
Vascularity	Well vascularized	8 (17%)
	Poorly vascularized	40 (83%)

US, ultrasound. The size of one tumor could not be measured because it was too large. size was denoted as the average.

as well vascularized. In contrast, if only one or two vessels were detected, the lesions were regarded as poorly vascularized. The enhancement patterns were classified into homogeneous enhancement and heterogeneous enhancement. Moreover, lesions with heterogeneous enhancement were further divided into those with obvious enhancement, moderate enhancement, slight enhancement, and unenhancement.

3. Results

3.1. US imaging findings

Forty-eight patients with primary AciCC of the parotid gland underwent preoperative US. Table 2 summarizes their US findings. The average (±SD) tumor size of 47 patients was 2.2 ± 0.63 cm (range, 1.2–3.7 cm); one tumor was too large to be measured. With regard to their morphological characteristics, 29 (60%) lesions had an irregular shape and 19 (40%) lesions had a regular shape. Moreover, 38 (79%) had a well-defined border, while 10 (21%) lesions had an ill-defined border. With regard to their echogenicity, 35 (73%) lesions were hypoechoic (Fig. 1), 1 (2%) lesion was isoechoic,
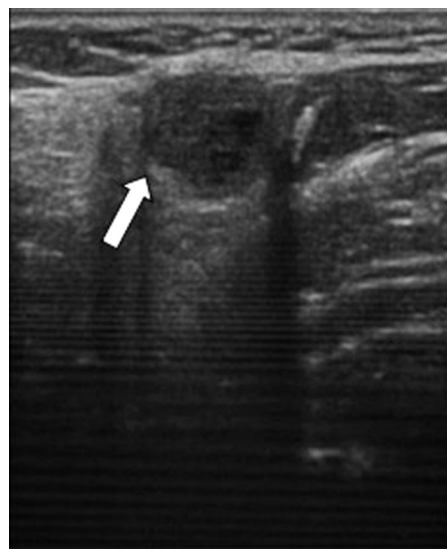

Fig. 1. Gray-scale ultrasound of a 57-year-old woman in the left parotid gland shows an irregular (lobular), well-defined, hypoechoic, heterogeneous mass (arrow), without acoustic enhancement.